

# Particle-Filtering-Based State-of-Health Estimation and End-of-Life Prognosis for Lithium-Ion Batteries at Operation Temperature

Daniel Pola<sup>1</sup>, Felipe Guajardo<sup>1</sup>, Esteban Jofré<sup>1</sup>, Vanessa Quintero<sup>1</sup>, Aramis Pérez<sup>1</sup>, David Acuña<sup>1</sup> and Marcos Orchard<sup>1</sup>

<sup>1</sup> *Department of Electrical Engineering, Faculty of Physical and Mathematical Sciences, Universidad de Chile, Santiago, Chile*

*daniel.pola@ing.uchile.cl*

*felipe.guajardo.m@ing.uchile.cl*

*esteban.jofre@ing.uchile.cl*

*vquintero@ing.uchile.cl*

*aramis.perez@ing.uchile.cl*

*davacuna@ing.uchile.cl*

*morchard@ing.uchile.cl*

## ABSTRACT

We present the implementation of a particle-filtering-based framework that estimates the State-of-Health (SOH) and predicts the End-of-Life (EOL) of Lithium-Ion batteries, efficiently incorporating variations of ambient temperature in the analysis. The proposed approach uses an empirical state-space model, in which inputs are explicitly defined as the average temperature of operation and the output of an external module that detects self-recharge phenomena, on the other hand the output is a function that relates the current SOH and temperature with the Usable Capacity in that cycle. In addition, this approach allows to deal with data losses and outliers. In order to correct erroneous initial conditions in state estimates, an Outer Feedback Correction Loop is implemented. Finally, this framework is validated using degradation data from four sources: experimental degradation data from two Li-Ion 18650 cells, accelerated degradation data openly provided by NASA Ames Research Center, and artificially generated degradation data at different ambient temperatures.

## 1. INTRODUCTION

Lithium-ion batteries are used to power different electric devices and power systems due to their high energy density, wide temperature operation range, no memory effects, among other characteristics (Ranjbar, Banaei, Khoobroo, & Fahimi, 2012). In applications like electric vehicles or micro-grids is important to know how the battery ages given its importance in system design as it is directly related to its lifespan; and to predict its EOL in order to make assertive decisions about the

time for replacement, preventing possible failures caused by unsatisfied power or energy requirements.

State-of-Health is a concept associated to how aged a battery is. It indicates the amount of energy that the battery can store or deliver respect to its initial capacity (Berecibar, Devriendt, et al., 2016). However there is no consensus in the scientific community on how the SOH should be determined, in fact it can be characterized by the internal impedance, capacity fade, power fade and/or self discharge time (Berecibar, Gandiaga, et al., 2016). In some Energy Storage Devices (ESD), specifically in Li-Ion batteries, SOH can not be directly measured. It has to be estimated from other observed variables such as the voltage in terminals, current drained from the battery, or its temperature. Besides, the SOH is affected by various related factors that take place at similar timescales, such as the DOD (Depth-of-Discharge), discharge current, charging regimen, and cell temperature (Moreira, Nascimento, & Rodrigues, 2012), (Drouilhet & Johnson, 1997). Moreover, the analysis of the degradation process requires the incorporation of predictive tools for the implementation of a scheme capable of performing simultaneously filtering (analysis of current state) and prognosis (analysis of future behavior) of the SOH. These prognostic models need to incorporate the capability of parameter adaptation to minimize the effect of measurement inaccuracies on erroneous SOH estimates, as well as incorporating changes in environmental and operating conditions within long-term predictions (Saha & Goebel, 2009), (Orchard, Tang, Saha, Goebel, & Vachtsevanos, 2010), (Pascoe & Anbuky, 2004).

SOH estimation has been studied using diverse approaches, one of the simplest solution is the Coulomb counting method (Ng, Moo, Chen, & Hsieh, 2009). However, due to the cumulative error that it carries it is highly accuracy sensitive. Other

---

Daniel Pola et al. This is an open-access article distributed under the terms of the Creative Commons Attribution 3.0 United States License, which permits unrestricted use, distribution, and reproduction in any medium, provided the original author and source are credited.

way of determining the SOH is by estimating the actual value of the battery internal impedance. For example, using Electrochemical Impedance Spectroscopy (EIS), which is a non-invasive method, is possible to characterize the impedance through a wide frequency spectrum with the limitation that measurements are noisy, and requires expensive equipment, usually found only in laboratories, restricting its application in practice (Saha & Goebel, 2009), (Dalal, Ma, & He, 2011). Also, researches on SOH estimation have focused on modeling the electrochemical behavior of the accumulators (Pattipati, Sankavaram, & Pattipati, 2011), (Santhanagopalan, Zhang, Kumaresan, & White, 2008), building equivalent circuits, or studying the relationship between ESD degradation and a set of specific features (SOC, DOD, or the accumulator age). Besides, fuzzy models and neural networks have also been used to estimate the SOH of Li-Ion batteries (Andre, Nuhic, Soczka-Guth, & Sauer, 2013), although both approaches present inaccuracies originated from uncertainty sources that are present in nonlinear systems. Furthermore, suboptimal Bayesian estimation techniques such as the Extended Kalman Filter (EKF) have been implemented for SOH prognosis. The problem arises when trying to propagate this estimate in time (n-step ahead predictions), since approximation errors are too significant to be neglected (Orchard & Vachtsevanos, 2009). In (Wei, Williard, Osterman, & Pecht, 2011), the concept of Bayesian estimation combined with Monte Carlo methods is used to update the parameters of an empirical model, thus representing the prediction of the degradation process via Probability Density Functions (PDF).

Sequential Monte Carlo methods represent a concrete opportunity for algorithm improvement, since they have proved to be useful when trying to represent uncertainty in the prognosis of other nonlinear degradation processes (Orchard & Vachtsevanos, 2009), (Orchard et al., 2010). Some ESD (e.g., Li-ion batteries) however, suffer sudden regeneration (or self-recharge) phenomena (Orchard et al., 2010), (Saha & Goebel, 2009), that directly affects the precision and accuracy of that type of algorithms. The statistical characterization of those phenomena has been incorporated within non-linear stochastic state-space models for SOH prognostic frameworks based on sequential Monte Carlo methods in (Olivares, Cerda, Orchard, & Silva, 2013), but neglecting the effect of an important variable, the operation temperature of the ESD.

Despite of the existence of Li-Ion battery degradation models that include the operation temperature as an input (Thomas et al., 2003), most of the described techniques consider an invariant temperature of approximately 296[K]. Fluctuations on the ambient or battery's temperature affect directly the chemical reaction rate. As the temperature ascends the internal impedance decreases and the capacity increases (Jeon & Baek, 2011), (Mommaa, Matsunaga, Mukoyama, & Osaka, 2012), resulting in a modification of the amount of energy that it can store or deliver in a cycle leading to erroneous

estimations and predictions of the SOH. Thus, the purpose and contribution of this work is to propose a Particle-Filtering (PF) scheme to estimate and predict the SOH of a Li-Ion battery, considering explicitly its temperature of operation in the state-space model developed in (Olivares et al., 2013).

## 2. PARTICLE FILTERING ESTIMATION ALGORITHM

Particle filters are sequential Monte Carlo methods used to represent analytically complex or unknown PDFs with sample-based representations. This task is done by generating a set of  $N \gg 1$  weighted particles  $\{w_k^{(i)}, x_{0:k}^{(i)}\}_{i=1 \dots N}$ ,  $w_k^{(i)} > 0, \forall k \geq 1$ , which represent random samples of a target distribution  $\pi_k$  and fulfill Eq. (1) in probability, where  $\phi_k$  is any  $\pi_k$ -integrable function (Arulampalam, Maskell, Gordon, & Clapp, 2002) (Andrieu, Doucet, & Punskeya, 2001). In this case  $\pi_k$  is chosen as the *posterior* distribution of the state vector  $p(x_{0:k}|y_{1:k-1})$  given the noisy observations  $y_{1:k}$

$$\sum_{i=1}^N w_k^{(i)} \phi_k(x_{0:k}^{(i)}) \xrightarrow{N \rightarrow \infty} \int \phi_k(x_{0:k}) \pi_k(x_{0:k}) dx_{0:k} \quad (1)$$

For the estimation stage this method has two well defined steps: prediction and update. In the prediction step the available states for every particle  $x_{0:k-1}^{(i)}$  are extended with their position in the next iteration  $\tilde{x}_k^{(i)}$  that distributes as an arbitrary importance distribution  $q((x_{0:k-1}, \tilde{x}_k)|x_{0:k-1})$  which is chosen as the *a priori* PDF  $p(\tilde{x}_k|x_{0:k-1})$  represented by the state transition function of the state-space model, minimizing the variance of the particle weights (Andrieu et al., 2001). Then, in the update step, the weights of the particles are modified from the measurement likelihood  $w_k^{(i)} \propto w_{k-1}^{(i)} \cdot p(y_k|\tilde{x}_{0:k})$  where  $\sum_{i=1}^N w_k^{(i)} = 1$ . This lets us approximate the *posterior* PDF ( $\pi_k$ ) of the state vector in the time  $k$  (Andrieu et al., 2001) by the Eq. (2).

$$\pi_k(x_k) = \sum_{i=1}^N w_k^{(i)} \cdot \delta(x_k - \tilde{x}_k^{(i)}) \quad (2)$$

Prognosis schemes can be understood as the result of long-term predictions describing the evolution of a fault indicator (in this case the SOH), with the purpose of estimate the Remaining Useful Life (RUL) of a component or system, taking as initial condition the particle population from estimation stage and projecting them in time without new observations. Then, it is possible to describe the evolution in time of the fault indicator through n-step-ahead predictions of a non-linear state-space model, representing the uncertainty of the process by a kernel function, shown in Eq. (3).

$$\tilde{p}(x_{k+m}|\tilde{x}_{0:k+m-1}) \approx \sum_{i=1}^N w_{k+m-1}^{(i)} K(x_{k+m} - E[x_{k+m}^{(i)}|\tilde{x}_{k+m-1}^{(i)}]) \quad (3)$$

Where  $E(\cdot)$  represents the expectation of a random variable and  $K(\cdot)$  is a kernel density function, which can be chosen as the process noise PDF, a Gaussian kernel, or a rescaled version of the Epanechnikov kernel (Orchard & Vachtsevanos, 2009)(Orchard, Tobar, & Vachtsevanos, 2009). Furthermore, we use a regularized version of this PF-based approach that characterizes the distribution of the predicted state vector by the position of the particles instead of their weights. As a result, the predicted state PDF in the time instant  $k + m$  is always represented by  $N$  particles  $x_{k+m}^{(i)*} = x_{k+m}^{(i)} + h_{opt} D_{k+m} \epsilon^{(i)}$ , ( $i = 1, \dots, N$ ), where  $h_{opt}$  is the optimal bandwidth of the kernel  $K(\cdot)$  and  $D_{k+m}$  is the square root of the empirical covariance of the predicted state in  $k + m$ .

The resulting predicted state PDF contains critical information about the evolution of the fault dimension over time. One way to represent that information is through the computation of statistics such as the probability of failure at some future time instant (EOL PDF), that is calculated as the Acuña's Time-of-Failure probability measure (Acuña, 2016). Another statistic is the Just In Time Point ( $JITP_{\gamma\%}$ ), that corresponds to the time instant  $k$  in which the cumulative probability of failure is  $\gamma\%$  as shown in Eq. (4), gives information in order to make decisions with failure risk considerations. Then, failure conditions may be defined through the determination of hazard zones (Orchard & Vachtsevanos, 2009), either using historical data or knowledge from process operators. The simplest case is where the concept of failure implies the instant when the fault feature crosses a given threshold. In that case, the probability of failure, conditional to the state, is equal to one if the state is exactly on the manifold that defines the threshold value.

$$JITP_{\gamma\%} = \underset{k}{\operatorname{argmin}} (Pr\{EOL \leq k\} \geq \gamma\%) \quad (4)$$

### 3. MODEL PROPOSAL FOR A SOH PROGNOSIS SCHEME AT A REFERENCE TEMPERATURE

Modeling the degradation of an ESD is a complex task, due to the amount of variables involved on the battery aging and their interaction (Vetter et al., 2005), (Barré et al., 2013). Specifically, the existence of parameters that depend on (i) Operational conditions as the magnitude of the current drained from the battery or the ambient temperature; and (ii) the chemistry of the electrodes and the electrolyte. Thus, an electrochemical approach may result in a very com-

plex model, increasing both the amount of parameters to deal with, and computational costs of the algorithm. Instead, this work proposes an empirical state-space non-linear model to describe the evolution of the degradation of a Li-Ion battery considering the effect of the temperature of operation explicitly.

In (Olivares et al., 2013) an empirical state space model was proposed to represent a regeneration phenomena that affects the battery. Equations (5) - (8) show the proposed SOH estimation and prognosis state-space model. This model was upgraded with inclusion of the average temperature of operation as a model input. The explicit inclusion of that variable in the model is needed in order to consider the amount energy that a battery can store and deliver. The neglect of this input variable may lead to wrong decisions if they are based solely on the observed capacity for the current cycle.

#### State transition equations:

$$x_1(k+1) = x_1(k)(\eta + x_2(k)) + \omega_1(k) \cdot \Phi(T(K)) \quad (5)$$

$$x_2(k+1) = x_2(k) + \omega_2(k) \quad (6)$$

$$x_3(k+1) = \delta(U(k))\omega_{31}(k) + \delta(1 - U(k))(x_3(k) \dots \dots \omega_{32}(k)) + \delta(2 - U(k))(x_3(k) + \omega_{31}(k)) \quad (7)$$

#### Measurement equation:

$$y(k) = C_{use}(x_1(k), T(k)) + (\delta(1 - U(k)) + \dots \dots \delta(2 - U(k))) \cdot x_3(k) + v(k) \quad (8)$$

The state  $x_1(k)$  is a capacity measure of the battery in  $[Ah]$  at a reference temperature  $T_{ref}$ .  $\Phi(T)$  is a function added to include the effect of the operation at a temperature different to  $T_{ref}$ .  $\eta$  is an efficiency parameter (Huggins, 2008) that explains how much energy is expected for a cycle given the capacity delivered in the previous one. The degradation tendency  $\eta$  is the portion of the energy delivered or stored in the last cycle that is expected to be delivered in the current one, this parameter is heavily affected by very high and low temperatures. Nevertheless within a certain temperature range, the operating temperature does not change the tendency of degradation in just a few cycles (Zhou, Qian, Allan, & Zhou, 2011) and therefore it can be considered constant. In order to deal with the differences between the assumed  $\eta$  and the actual degradation trend, state  $x_2(k)$  is added as an unknown parameter under the concept of artificial evolution (Orchard & Vachtsevanos, 2009). The state  $x_3(k)$  is associated with the additional available energy due to regeneration phenomena and allows the inclusion of the extra capacity only in the observation equation and not in  $x_1$ . Function  $\delta(\cdot)$  is the Kronecker delta and  $U(k)$  is an on-line PF-based regeneration phenomena detection module developed in (Olivares et al., 2013) described in the Eq. (9). It is worth to mention that to

obtain a true value of the SOH (by the common definition in percentage) it is necessary to divide the state  $x_1$  by the nominal capacity of the battery, or in the absence of this value by the capacity delivered at the first cycle of operation (assuming a valid first measurement).

$$U(k) = \begin{cases} 0 & \text{self-recharge does not exist,} \\ 1 & \text{self-recharge is detected at cycle } k \\ & \text{or self-recharge is fading,} \\ 2 & \text{additional self-recharge is} \\ & \text{detected before the latest one fades.} \end{cases} \quad (9)$$

Process noises  $\omega_1$  and  $\omega_2$ , and observation noise  $v$  are zero-mean Gaussian noise terms;  $\omega_1$  is augmented during the first iterations of the algorithm by the effect of an outer feedback correction loop to deal with erroneous initial condition for  $x_1$  according to (Orchard et al., 2009).  $\omega_{31}$  is a log-normal noise used to characterize the typical amount of SOH that is added in the event of successive regeneration phenomena;  $\omega_{32}$  is used to characterize the typical damping ratio of self-recharge phenomena and distributes as a uniform over a range. Both  $\omega_{31}(k)$  and  $\omega_{32}(k)$  were determined statistically in (Olivares et al., 2013) studying the accelerated degradation data provided by NASA Ames Prognostic Center of Excellence.

Measurement Eq. (8) represents the measured capacity of the battery ( $y(k)$ ) as the sum of (i) the Usable Capacity  $C_{use}$  (Lam, Bauer, & Kelder, 2011), that is the capacity that the battery can deliver or store in the  $k^{th}$  cycle at a given SOH and average temperature  $T(k)$  and (ii) the extra capacity added by the self-regeneration phenomena  $x_3$ .  $C_{use}$  is defined by the Vogel-Tammann-Fulcher (VTF) equation suggested in (Lam et al., 2011) and shown in Eq. (10). This function establishes a relation between the Usable Capacity at certain temperature  $T(k)$  and the capacity of the battery  $x_1$  at a reference temperature  $T_{ref}$ .  $\alpha$  and  $\beta$  are parameters that have to be fitted using the capacity and the temperature data.

$$C_{use}(x_1, T) = x_1 \cdot e^{\alpha \left( \frac{1}{T-\beta} - \frac{1}{T_{ref}-\beta} \right)} \quad (10)$$

The evolution of the Usable Capacity of a battery should be described by Eq. (11). Then, using the latter in Eq. (10) and dividing by the exponential term, the equation Eq. (5) is found, where the term  $\Phi(T)$  is explicitly showed in Eq. (12).

$$C_{use}(x_1(k+1), T(k)) = C_{use}(x_1(k), T(k)) \times \dots \quad (11) \\ \dots (\eta(T(k)) + x_2(k)) + \omega_1(k)$$

$$\Phi(T) = e^{-\alpha \left( \frac{1}{T(k)-\beta} - \frac{1}{T_{ref}-\beta} \right)} \quad (12)$$

An important assumption made for this work is that the adjustment established in Eq. (10) is invariant with cycling and

time, but as the internal impedance increases with a lower SOH, it may be expected that the values of  $\alpha$  and  $\beta$  change when the battery has degraded. In this regard, a complete study of the batteries should include characterization of this relation for several different states of degradation.

#### 4. ISSUES RELATED TO THE IMPLEMENTATION OF THE PARTICLE-FILTERING-BASED SOH PROGNOSIS SCHEME

Particle filtering algorithms are a suitable option to work with non-linear and not necessarily Gaussian models, and to represent the uncertainty of the system in the prognosis stage. In this regard, the SOH prognosis is achieved with a particle-filtering-based scheme using the model proposed.

##### 4.1. Configuration of the Particle Filter Algorithm

The formulation of PF-based prognostic approaches has been widely covered in literature (Saha & Goebel, 2009), (Orchard & Vachtsevanos, 2009), (Dalal et al., 2011). However, there are specific issues associated to the implementation of these schemes that depend, in a strong manner, on the number of states of the dynamic system and the type of non-linearities exhibited by them. In order to determine the value of the parameters for the SOH prognosis scheme, it is required to compare the performance of this suboptimal scheme with respect to an analytic solution; a complex task given the non-linearities of the considered model. For this reason, a reasonable method to set the filter parameters is the one adopted in (Olivares et al., 2013), where a simplified scenario is used to determine an adequate configuration of the PF algorithm by using a linear Gaussian dynamic system. With this methodology the performance of the proposed PF-based SOH prognosis framework is compared versus the optimal solution given by the *a priori* prediction equations of the Kalman filter. Since the model proposed in this work is generated from the one used in (Olivares et al., 2013), it is considered that those results are appropriate for this work. The configuration is: (i) 50 particles, (ii) 40 realizations of the non-linear filter, and (iii) 50 realizations of the long-term predictions. The value of 50 particles is the lower amount that presents a similar result as the analytic solution. Thus, an increment in the number of particles does not affect the performance of the scheme. To facilitate the calculation of confidence intervals of 95% and integer percentage values of a resulting *a posteriori* distribution (e.g. 99%), the number of particles is duplicated to 100. With that number, the execution of the SOH estimation and prognosis procedures takes less than 1.5[sec] using the MATLAB environment and a Intel Core<sup>(TM)</sup> i7 CPU (3.07GHz) and 16GB of RAM.

## 4.2. Dealing with Outliers and Loss Data

Since the degradation process of lithium-ion batteries happens during an extended period of time, one may expect error in the data, either from lost data or outliers. Erroneous data may affect the performance of the filtering stage and result in a wrong assumption of a degraded battery. The approach used to operate with this type of data is designed to execute the prognosis stage, while data is missing or is considered as an outlier; by using the previous cycle number as the prediction time and the corresponding value of the state vector to begin the prediction. At the time instant when new data is valid and available (measured capacity and temperature of operation of the cycle), the filtering stage restarts with the state values of the last prediction time instant.

To determine whether a new measurement is an outlier or not, a hypothesis test is applied to compare the *a priori* observation equation with respect to the measured capacity, both transformed to a value at a reference temperature according to Eq. (10). The null hypothesis  $H_0$ , corresponding to a new measurement that is valid, is characterized by the *a priori* one-step-ahead prediction of the system output PDF. The false alarm probability ( $p_{fa}$ ) is set to 1%. This test uses a time-varying threshold  $\Theta_{th}(k)$  that depends on the position of the state particles, defined as the difference between a scalar  $\Theta_y(k)$  and a constant  $K_{th}$  (a 12% of the nominal capacity). The scalar is obtained from the particles that satisfies  $\Sigma\omega^{(i)}(k) > p_{fa}$  and  $h(x^{(i)}(k)) > \Theta_y(k)$  (being  $h(x)$  the measurement Eq. (8)), resulting in  $\Theta_{th}(k) = \Theta_y(k) - K_{th}$ . That is, the null hypothesis is rejected if the measurements are a fixed amount below most of the particles' position. This test is illustrated in Figure 1 for a continuous PDF and  $p_{fa}$  of  $\alpha\%$ .

## 4.3. Data

The proposed scheme is validated using data from four different sources. The first data used (DS1) was provided by NASA Ames public datasets. It consists of a battery exposed to an accelerated degradation at 296[K] (Saha & Goebel, Visited: Oct.2007). Furthermore, cycles 19 to 23 were deleted and the

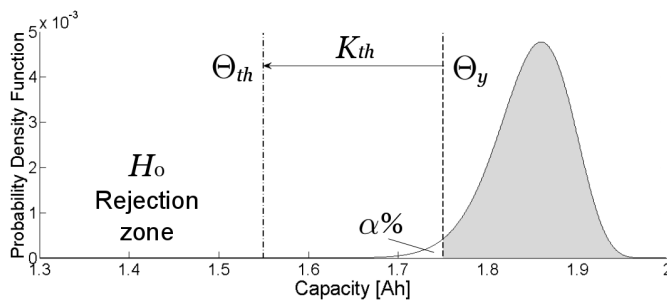


Figure 1. Illustration of the PF-based hypothesis test for outlier detection.

value of cycles 60 to 62 were changed for 1, 3[Ah] in order to test the outlier detection module. The second and third datasets were generated on two 18650 Li-ion rechargeable batteries (3, 7[V] and 2400[mAh]) using an adaptation of the Federal Urban Driving Schedule (FUDS) battery power profile (United States Advanced Battery Consortium, 1996) at different temperature of operation: low temperature, around 276[K] (DS3, see Figure 2) and ambient temperature, around 296[K] (DS2, see Figure 3).

Finally, an artificial data set (DS4) was created based on the data of DS1, but considering different operating temperatures for each cycle. The SOH estimation and prognosis scheme requires, for each cycle, the average temperature of operation, the measured capacity, and the parameters  $\alpha$  and  $\beta$  that satisfy in Eq. (10). With these values, an equivalent capacity at a reference temperature  $T_{ref}$  can be obtained. To generate DS4, the process is reversed using the values of  $\alpha$  and  $\beta$  obtained for the cells tested in the laboratory. Then, creating an arbitrary temperature set with values fluctuating between 275[K] and 298[K], a capacity measurement is made using the transformation Eq. (10) over capacity data at 298[K]. A random noise is added to the new capacity measurements to include uncertainty associated to the characterization. Figure 4 shows the resulting generated capacity measurement at different temperatures.

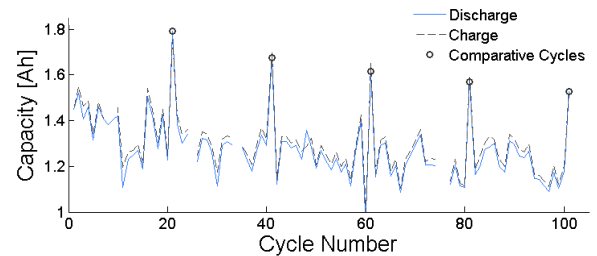


Figure 2. Degradation data obtained cycling Li-Ion 18650 Battery at low temperature (DS3).

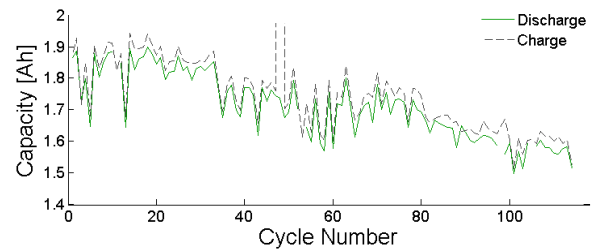


Figure 3. Degradation data obtained cycling Li-Ion 18650 Battery at room temperature (DS2).

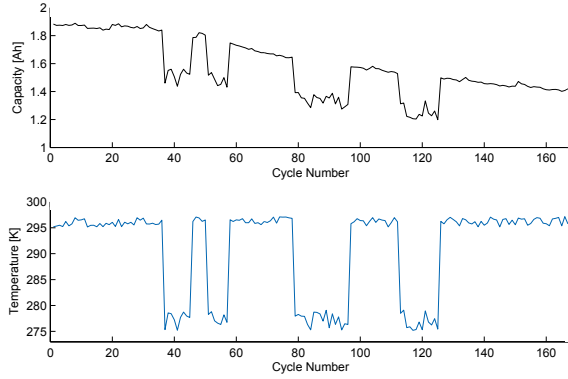


Figure 4. Artificial generated degradation data (DS4)

## 5. VALIDATION AND RESULTS

The main purpose of the proposed state-space model is to work the degradation data at a reference temperature ( $T_{ref}$ ). Therefore, the long-term predictions of the state vector are conducted at  $T_{ref}$  using the results of the filtering stage as the initial condition. Then, we can obtain a probabilistic characterization of the EOL of the battery, by finding the time instants when the trajectory of the particles (at  $T_{ref}$ ) reaches a given percentage of capacity loss. This section illustrates the performance of the SOH PF-based prognosis scheme for done realization of the non-linear filter, and one realization of the long-term prediction.

Figures 5, 6 and 7 present the results of one realization of the prognosis scheme for DS1. The initial condition of the particles of  $x_1$  are set around  $1[Ah]$  in order to include an erroneous initialization. In this experiment in particular, the failure threshold was diminished to a 65% of the nominal capacity to illustrate in a better manner the proposed scheme dealing with regeneration phenomena and lost data.

Figure 5 shows the validation data (bold black line), state  $x_1$  estimation (orange line), the observation of the model (dashed green line), and long-term predictions (dashed bold blue line). All of them are presented at reference temperature of  $296[K]$ . In addition, red circles show the cycles where the detection signal of the regeneration phenomena detection module is non-null. Gray lines correspond to predictions of the particles of the state  $x_1$ , and segmented magenta lines represent the confidence interval of 95%. This result illustrates how the outer feedback correction loop allows  $x_1$  to converge to a reasonable value given the observations, and allows the scheme to work properly even with an erroneous initialization of  $x_1$ . The prediction instant is the  $107^{th}$  cycle (dark vertical segmented line), but some predictions can be seen between cycles 19 to 23 and 60 to 62 due to the outlier detection module. The latter is important when working with non-ideal data. The evolution of  $x_2$  is presented in Figure 6, exhibiting predictions of the state vector during the filtering

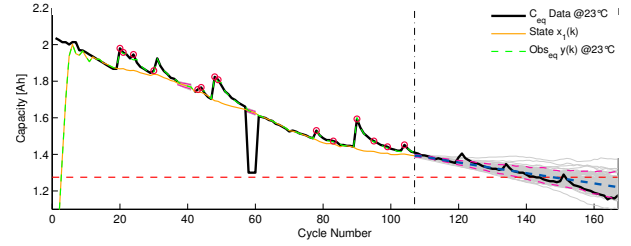
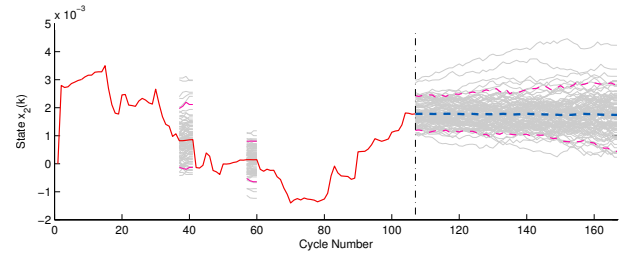
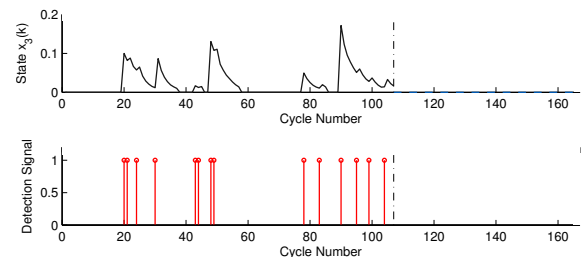


Figure 5. SOH estimation and prognosis for DS1 using the proposed PF-based framework.

Figure 6. Evolution of the state  $x_2$  for DS1 using the proposed PF-based framework.

stage. Figure 7 shows the detection signal of the regeneration phenomena (the evolution of  $x_3$  that explains the difference between the observation equation and  $x_1$  during the filtering stage), after the prediction time it is assumed that  $x_3 = 0$ . Finally, the ground truth EOL is in the cycle 143, and the expected EOL is in the cycle 147 for a 40-cycle prediction window. However, this example is just one illustrative realization of the SOH prognosis scheme.

Figures 8 and 9 show the evolution of  $x_1$ , the observation, and the measurement data (analogous to the Figure 5) for the laboratory generated degradation data DS2 and DS3 respectively. For those noisy sets, the self-regeneration detection module not only works with its original purpose, but also for high capacity peaks that last one or two cycles, making the SOH to evolve smoothly. From the perspective of a risk-based decision, it is not critical to have the regeneration

Figure 7. Evolution of the state  $x_3$  and the Detection Signal for DS1 using the proposed PF-based framework.

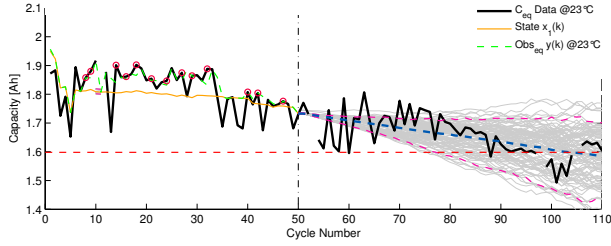


Figure 8. SOH estimation and prognosis for DS2 using the proposed PF-based framework.

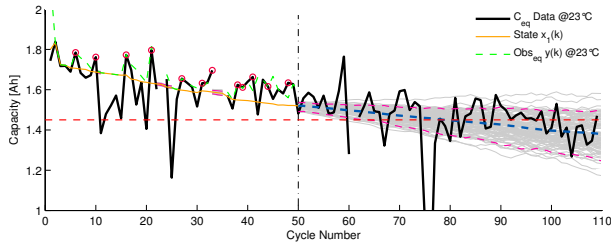


Figure 9. SOH estimation and prognosis for DS3 using the proposed PF-based framework.

detection module working in that manner, because it may result in an underestimation of the SOH most of the time. The noisy behavior of these data set makes difficult to establish the time instant of the ground truth EOL, but for DS2 the predictions can be compared with data post cycle 85. To evaluate the long-term predictions of  $x_1$  the ground truth EOL value can be set at  $1.598[Ah]$  at cycle 95. The expectation of the SOH crosses the EOL threshold at the  $104^{th}$  cycle as shown in Figure 8.

The results of the long-term predictions of  $x_1$  for the artificial degradation set DS4 are presented Figure 10. This data set is used to evaluate the operation of the proposed scheme with a time varying temperature of operation. As one may observe, the scheme produces both the estimations and predictions of the state  $x_1$  at a reference temperature, allowing the application of the outer-feedback correction loop and the self-regeneration detection module over temperature varying degradation data.

Since the proposed approach is based on realizations of estimated PDF and includes the uncertainty of the model by random processes, the prediction results of the  $JITP$  and the expected EOL ( $E\hat{O}L$ ) may vary from one realization of the whole process to another. In order to characterize these differences with statistics, 100 realizations of the estimation-prognosis process were performed for every data set. Table 1 shows the mean of  $E\hat{O}L$ , the 95% of Confidence Interval (CI) limits, defined by  $JITP_{2.5\%}$  to  $JITP_{97.5\%}$ , the mean of the  $JITP_{15\%}$ ,  $JITP_{5\%}$ . The ground truth value of the EOL is assumed when the SOH reaches an 80% of the initial

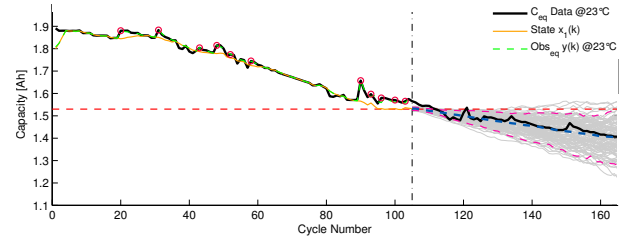


Figure 10. SOH estimation and prognosis for DS4 using the proposed PF-based framework.

condition (equally, when the state  $x_1$  drops below the 80% of the initial condition). In Table 1 it can also be seen that the ground truth EOL lies within the 95% confidence interval, and the mean of  $JITP_{\gamma\%}$  for  $\gamma = 5\%$  and  $= 15\%$  occurs before the ground truth EOL, which is a desirable behavior in applications where a battery failure is unacceptable.

Figure 11 shows the EOL PDF during one realization of the prognosis stage for DS1, calculated with the Acuña Time-of-Failure probability measure (Acuña, 2016). Here also, it is shown graphically the 95% of CI limits defined by cycles 96 and 107, and the  $E\hat{O}L$  calculated is equal to cycle 101.59.

## 6. CONCLUSION

In this work an empirical state-space-based particle filtering framework is proposed to describe the evolution of the degradation of ESD's, specifically in Li-Ion cells, with an explicit inclusion of the mean value of the operation temperature. The proposed model consists of three estates which are (i) SOH at a reference temperature of  $296[K]$  (ii) an added unknown parameter under the concept of artificial evolution and (iii) the extra capacity available caused by self regeneration phenomena. The proposed approach uses an outer feedback correction loop that increases the noise associated to state  $x_1$  in the first iterations so it can converge to a reasonable value in pres-

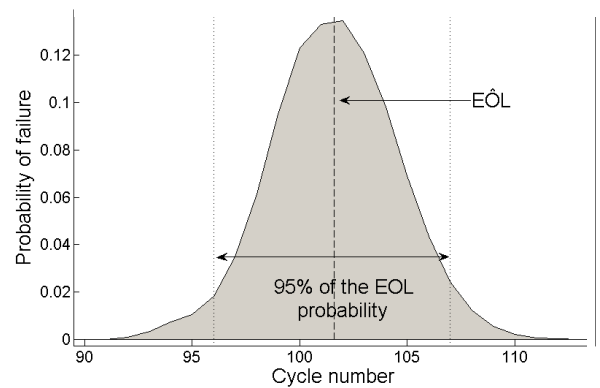


Figure 11. EOL PDF for one realization of the scheme for DS1

Table 1. Mean results from 100 realizations of the proposed scheme

DS#	EOL [cycle]	$\hat{EOL}$ [cycle]	95% CI [cycle]	$JITP_{5\%}$ [cycle]	$JITP_{15\%}$ [cycle]
2	114	127.9	[109.9 145.6]	112.7	118.4
3	87	80.6	[73.1 88.2]	74.1	76.4
4	114	105.8	[97.2 114.5]	98.5	101.1

ence of erroneous initial conditions. To work with outliers or lost data an hypothesis-test-based module is included in the estimation stage. When a new measurement is considered invalid, then the algorithm is able to generate predictions about the state vector, restarting the filtering stage when a new available measurement is valid. The proposed model includes an important factor of the batteries phenomenology: the operation temperature. The concept of *Usable Capacity* makes possible to include the average temperature of operation during a cycle as an external input to the degradation model. As a consequence, the SOH estimation and prognosis are conducted at a reference temperature. This result is important because it allows to handle temperature-varying degradation data, and make long-term predictions at a nominal temperature. This scheme is validated using public available and laboratory-generated degradation data, but for a complete validation degradation data from different li-ion batteries with different operation temperatures and changes of this during their lifetime is required. Since the generation of battery degradation data at different temperatures is a slow procedure (even more with the absence of an automatic cycling equipment and a temperature chamber), an artificially generated data set is introduced to test the performance of the scheme. This scheme allows to prognosticate the SOH of a battery at a reference temperature, generating a conditional PDF of  $x_1$  for each future cycle. The latter allows to obtain indicators as confidence intervals, expectations or *JITP*.

#### ACKNOWLEDGEMENT

This work has been partially supported by FONDECYT Chile Grant Nr. 1140774, and the Advanced Center for Electrical and Electronic Engineering, AC3E, Basal Project FB0008, CONICYT. The work of Daniel Pola was supported by FONDECYT Chile Grant Nr. 1110070 and CONICYT-PCHA/Magister Nacional/2013-221320011. The work of Aramis Pérez was supported by the University of Costa Rica (Grant for Doctoral Studies) and CONICYT-PCHA/Doctorado Nacional/2015-21150121. The work of Vanessa Quintero was supported by the Universidad Tecnológica de Panama and IFARHU (Grant for Doctoral Studies) and CONICYT-PCHA/Doctorado Nacional/2016-21161427.

#### NOMENCLATURE

DOD	Depth-of-Discharge
EIS	Electrochemical Impedance Spectroscopy
EKF	Extende Kalman Filter
EOL	End-of-Life
ESD	Energy Storage Devices
FUDS	Federal Urban Driving Schedule
PDF	Probability Density Functions
RUL	Remaining Useful Life
SOH	State-of-Charge
VTF	Vogel-Tammann-Fulcher
JITP	Just In Time Point

#### REFERENCES

- Acuña, D. (2016). *Manejo de incertidumbre ante pérdida parcial o total de datos en algoritmos basados en métodos secuenciales de monte carlo y nueva definición de probabilidad de falla en el contexto de monitoreo en línea* (Unpublished master's thesis). Facultad de Ciencias Físicas y Matemáticas, Universidad de Chile, Santiago, Chile.
- Andre, D., Nuhic, A., Soczka-Guth, T., & Sauer, D. (2013). Comparative study of a structured neural network and an extended Kalman filter for state of health determination of lithium-ion batteries in hybrid electric vehicles. *Engineering Applications of Artificial Intelligence*, 26, 951-961.
- Andrieu, C., Doucet, A., & Punsakaya, E. (2001). Sequential monte carlo methods in practice. In A. Doucet, N. de Freitas, & N. Gordon (Eds.), (pp. 79–95). New York, NY: Springer New York. doi: 10.1007/978-1-4757-3437-9\_4
- Arulampalam, M. S., Maskell, S., Gordon, N., & Clapp, T. (2002, Feb). A tutorial on particle filters for on-line nonlinear/non-gaussian bayesian tracking. *IEEE Transactions on Signal Processing*, 50(2), 174-188. doi: 10.1109/78.978374
- Barré, A., Deguilhem, B., Grolleau, S., Gérard, M., Suard, F., & Riu, D. (2013). A review on lithium-ion battery ageing mechanisms and estimations for automotive applications. *Journal of Power Sources*, 241, 680-689.
- Berecibar, M., Devriendt, F., Dubarry, M., Villarreal, I., Omar, N., Verbeke, W., & Mierlo, J. V. (2016, July).

- Online state of health estimation on nmc cells based on predictive analytics. *Journal of Power Sources*, 320, 239250.
- Berecibar, M., Gandiaga, I., Villarreal, I., Omar, N., Mierlo, J. V., & den Bossche, P. V. (2016, April). Critical review of state of health estimation methods of li-ion batteries for real applications. *Renewable and Sustainable Energy Reviews*, 56, 572587.
- Dalal, M., Ma, J., & He, D. (2011). Lithium-ion battery life prognostic health management system using particle filtering framework. *Proceedings of the Institution of Mechanical Engineers, Part O: Journal of Risk and Reliability*, 225, 81-90.
- Drouilhet, S., & Johnson, B. (1997, January). A battery life prediction method for hybrid power applications. *Presented at the 35th AIAA Aerospace Sciences Meeting and Exhibit, Reno, Nevada*.
- Huggins, R. A. (2008). *Advanced batteries: Materials science aspects*. Springer-Verlag.
- Jeon, D. H., & Baek, S. M. (2011). Thermal modeling of cylindrical lithium ion battery during discharge cycle. *Energy Conversion and Management*, 52, 2973-2981.
- Lam, L., Bauer, P., & Kelder, E. (2011, October). A practical circuit-based model for Li-ion battery cells in electric vehicle applications. *Telecommunications Energy Conference (INTELEC), IEEE 33rd International*.
- Momma, T., Matsunaga, M., Mukoyama, D., & Osaka, T. (2012). AC impedance analysis of lithium ion battery under temperature control. *Journal of Power Sources*, 216, 304-307.
- Moreira, J., Nascimento, C., & Rodrigues, L. (2012). Health monitoring and remaining useful life estimation of lithium-ion aeronautical batteries. *IEEE*.
- Ng, K. S., Moo, C.-S., Chen, Y.-P., & Hsieh, Y.-C. (2009). Enhanced coulomb counting method for estimating state-of-charge and state-of-health of lithium-ion batteries. *Applied Energy*, 86(9), 1506 - 1511.
- Olivares, B., Cerda, M., Orchard, M., & Silva, J. (2013, February). Particle-filtering-based prognosis framework for energy storage devices with a statistical characterization of state-of-health regeneration phenomena. *IEEE Transactions on Instrumentation and Measurement*, 62, 364-376.
- Orchard, M., Tang, M., Saha, B., Goebel, K., & Vachtsevanos, G. (2010, September). Risk-sensitive particle-filtering-based prognosis framework for estimation of remaining useful life in energy storage devices. *Studies in Informatics and Control*, 19, 209-218.
- Orchard, M., Tobar, F., & Vachtsevanos, G. (2009, December). Outer feedback correction loops in particle filtering-based prognostic algorithms: Statistical performance comparison. *Studies in Informatics and Control*, 18, 295-304.
- Orchard, M., & Vachtsevanos, G. (2009). A particle-filtering approach for on-line fault diagnosis and failure prognosis. *Transactions of the Institute of Measurement and Control* 2009, 31, 221-246.
- Pascoe, P., & Anbuky, A. (2004). Standby vrla battery reserve life estimation. *Telecommunications Energy Conference INTELEC. 26th Annual International*, 516-523.
- Pattipati, B., Sankavaram, C., & Pattipati, K. (2011). System identification and estimation framework for pivotal automotive battery management system characteristics. *Transactions on Systems, Man, AND CYBERNETICS - PART C: APPLICATIONS AND REVIEWS*, 41, 869-884.
- Ranjbar, A., Banaei, A., Khoobroo, A., & Fahimi, B. (2012, March). Online estimation of state of charge in li-ion batteries using impulse response concept. *IEEE Transactions on Smart Grid*, 3(1).
- Saha, B., & Goebel, K. (2009). Modeling li-ion battery capacity depletion in a particle filtering framework. *Annual Conference of the Prognostics and Health Management Society, San Diego, CA*.
- Saha, B., & Goebel, K. (Visited: Oct.2007). *Battery data set*. <http://ti.arc.nasa.gov/tech/dash/pcoe/prognostic-data-repository>. (NASA Ames Prognostics Data Repository, NASA Ames, Moffett Field, CA)
- Santhanagopalan, S., Zhang, Q., Kumaresan, K., & White, R. E. (2008). Parameter estimation and life modeling of lithium-ion cells. *Journal of The Electrochemical Society*, 155, A345-A353.
- Thomas, E., Case, H., Doughty, D., jungst, R., Nagasubramanian, G., & Roth, E. (2003). Accelerated power degradation of Li-ion cells. *Journal of Power Sources*, 124, 254-260.
- United States Advanced Battery Consortium. (1996, January). Electric vehicle battery test procedures (Revision 2 ed.) [Computer software manual].
- Vetter, J., Novk, P., Wagner, M., C. Veit, K. M., Besenhard, J., Winter, M., ... Hammouche., A. (2005). Ageing mechanisms in lithium-ion batteries. *Journal of Power Sources*, 147, 269-281.
- Wei, H., Williard, N., Osterman, M., & Pecht, M. (2011). Remaining useful performance analysis of batteries. *IEEE Conference on Prognostics and Health Management (PHM)*, 1-6.
- Zhou, C., Qian, K., Allan, M., & Zhou, W. (2011, December). Modeling of the cost of EV battery wear due V2G application in power systems. *IEEE Transactions on Energy Conversion*, 26(4).

## BIOGRAPHIES

**Daniel Pola** received his B.S. and M.Sc. degrees in electrical engineering from the University of Chile in 2012 and 2014, respectively. His research interests include estimation and prognosis based on Bayesian algorithms, health management for energy storage devices, system identification, and control systems.

**Felipe Guajardo** was born in Santiago, Chile. He is currently working toward the B.S. degree in electrical engineering at the University of Chile, Santiago, Chile. His research interests include control strategies, machine learning and renewable energy.

**Esteban Jofré** was born in Santiago, Chile. He is currently working toward the B.S. degree in electrical engineering at the University of Chile, Santiago, Chile. His research interests include health management in energy storage devices and renewable energy.

**Vanessa Quintero** received her B.Sc degree from Electronics and Telecommunication Engineering at the Universidad Tecnológica de Panama (2007). Currently she is a doctorate student at the University of Chile. Her research interests include estimation, prognostics with applications to battery and protocols design

**Aramis Pérez** received his B.Sc. degree (2002), and Licentiate degree (2005) in Electrical Engineering, and the M.Sc degree (2010) in Business Administration from the University of Costa Rica. He is an electrical engineering doctorate student at the University of Chile. His research interests in-

clude parametric and non-parametric modeling, system identification, data analysis, machine learning, and manufacturing processes.

**David E. Acuña** was born in Santiago, Chile. He received his B.Sc. and M.Sc. degrees in Electrical Engineering from University of Chile in 2014 and 2016, respectively. He currently is pursuing a Ph.D. in the same university. His research interests include Bayesian filtering, uncertainty quantification, and prognostics and health management with applications on energy storage devices and aerospace.

**Marcos Orchard** received the B.S. degree and a Civil Industrial Engineering degree with electrical major from Catholic University of Chile. He also received the M.S. and Ph.D. degrees from The Georgia Institute of Technology, Atlanta, GA, USA. He is currently an Associate Professor with the Department of Electrical Engineering at Universidad de Chile. His current research interest is the design, implementation and testing of real-time frameworks for fault diagnosis and failure prognosis, with applications to battery management systems, mining industry, and finance.